Temperature Effect on *Listeria Monocytogenes* Planktonic Growth and Biofilm-Forming Ability

Joana Catarina Andrade[1]; Rita Bernardo[2]; António Salvador Barreto[3]; Telmo Nunes[4]; Ana Rita Henriques[5]*

[1]*MSc in Microbiology, University of Lisbon, Portugal.*

[2]*MSc in Microbiology, University of Lisbon, Portugal.*

[3]*PhD in Veterinary Sciences, Technical University of Lisbon, Portugal.*

[4]*MSc in Veterinary Public Health, Technical University of Lisbon, Portugal.*

[5]*PhD in Veterinary Sciences, University of Lisbon, Portugal.*

*Corresponding Author(s): Ana Rita Henriques

CIISA – Centre for Interdisciplinary Research in Animal Health, Faculty of Veterinary Medicine, University of Lisbon, Avenida da Universidade Técnica, 1300-477 Lisboa.

Tel: 00-351-213-652-834;

Email: anaritah@fmv.ulisboa.pt

Abstract

Listeria monocytogenes is an important foodborne pathogen with the capacity to grow at low temperatures and the ability to form biofilms. These features are particularly significant to food business operators producing ready-to-eat foods with a long refrigerated shelf-life not undergoing any listericidal treatment before consumption.

Objectives: This work aims to assess the temperature effect on L. *monocytogenes* growth in planktonic suspension and in mono-species biofilms.

Methods and results: Isothermal planktonic growth at 12°C and 37°C was assayed using viable cell counts and optical density measurements that revealed a strong positive correlation, confirming the reliability of combining both methods to estimate L. *monocytogenes* concentration. Experimental data were then fitted to Baranyi and Roberts primary predictive model and the estimated growth parameters confirmed that *μmax* at 37°C (0.375 ± 0.072 log cfu/ml/h) was higher than at 12°C (0.054 ± 0.001 log cfu/ml/h), with identical L. *monocytogenes* final concentrations which emphasizes its ability to grow at refrigerated temperatures. Experimental results from the isothermal growth assay and ComBase Predictor growth model were similar, with slightly higher estimated *μmax* (37°C: 0.480 log cfu/ml/h; 12°C: 0.068 log cfu/ml/h) in the predictor growth model. The studied strains demonstrated biofilm-forming ability at 12°C, 20°C and 30°C after 5 days of growth. No significant differences in biofilm formation at different temperatures were detected considering viable cell counts values, but when using crystal violet staining optical density results significant differences were found, with the highest formation occurring at 30ºC. A positive strong correlation was found between viable cell counts and crystal violet staining optical

density results. In fact, both methods complement each other, because while viable cell counts measures viable cells, crystal violet staining optical density considers total biomass (viable and non-viable cells and extracellular matrix components). Nevertheless, in this work all L. *monocytogenes* strains revealed to be weak biofilm producers.

Conclusion: Overall, this studys results contribute with important initial information on L. *monocytogenes* growth and biofilm formation to further assist predictive growth modeling in food matrices and environments, also enabling subsequent quantitative microbial risk assessment, to improve pathogen's control.

Introduction

Listeria monocytogenes is the causative agent of human listeriosis, an important foodborne disease with a high fatality rate particularly in new-born infants, pregnant woman, elderly and immunocompromised patients [1-3]. Listeriosis is almost entirely transmitted through the ingestion of contaminated foods [4].

The ability to colonize food environments, enduring an extensive variety of physicochemical conditions and different processing hurdles, is due to L. *monocytogenes* physiological and ecological traits [5,6].

After gaining access to a food facility, through incoming raw materials and ingredients, packaging materials, or even food handlers, L. *monocytogenes* is able to persist for months or years within the food premises, especially in food contact surfaces [7,8].

L. *monocytogenes* can adhere to different surfaces within the food industry, such as plastic, polypropylene, rubber, stainless steel, glass and produce biofilms [7,9]. In the biofilm, bacteria are embedded by an extracellular matrix able to function as a structural scaffold and defense barrier [8]. Once established, biofilms confer protection against harsh environmental conditions, enabling to sustain the survival of bacteria and tolerance to food environment related hurdles [10]. These persistent strains have been linked to recurring contamination of finished products [10-12]. Although this cross-contamination transfers low levels of L. *monocytogenes* onto food, its psychrotrophic nature enables growth during refrigerated storage, reaching levels that might represent an increased risk to the consumer [13-15]. This is even more concerning if temperature fluctuation occurs in any of the production and distribution stages, or even at the household level, and if the food is a ready-to-eat product, not requiring a listericidal treatment before consumption [16-18].

This work aims to assess L. *monocytogenes* growth in planktonic suspension and in mono-species biofilms, depicting food and food-producing environment conditions.

The resulting data in culture media and different temperatures will provide important initial information to further assist predictive growth modeling in food matrices and environments, also enabling subsequent quantitative microbial risk assessments.

Materials and methods

Selection and revival of L. *monocytogenes* strains

To account for variation in growth and survival among *Liste-*

ria monocytogenes strains and to have representatives of the three serogroups more frequently related to human disease, three reference strains were assessed: L. *monocytogenes* CECT 4031 (serogroup IIa), L. *monocytogenes* CECT 935 (serogroup IVb) and L. *monocytogenes* CECT 937 (serogroup IIb).

For strains' revival, stock cultures stored at -80°C in preservation cryotubes containing Brain Heart Infusion (BHI) broth (Scharlab, S.L, Barcelona, Spain) supplemented with 15% glycerol (Merck KGaA, Darmstadt, Germany) were thawed and 100 µl of inoculum was transferred into 5 ml of BHI broth. After 24 hours (h) of incubation at 37°C, a loop (10 µl) of inoculum was streaked onto BHI agar (Scharlab, S.L.) and incubated at 37°C for 24 h.

L. *monocytogenes* isothermal growth in BHI broth

An isolated colony of L. *monocytogenes* was suspended in 5 ml of BHI broth (Scharlab, S.B.). The suspension was incubated at constant temperature of 12° and 37 °C. Each sample was periodically examined to assess the growth of L. *monocytogenes*. For that, bacterial suspensions' optical density at 600 nm (OD_{600nm}) was measured on a spectrophotometer Ultrospec 2000 (Pharmacia Biotech, Cambridge, England) at regular time intervals. Together with OD_{600nm}, enumeration of viable bacterial cells (VCC) at regular time intervals was also performed. Three independent growth experiments were performed for each temperature condition (37°C and 12°C), in each of the considered sampling time points (Table 1).

Table 1: Sampling time points used to assess *L. monocytogenes* CECT 4031 growth in BHI broth at 37^0C and 12^0C.

Sampling time								
Incubation at 37°C				Incubation at 12°C				
2 h	10 h	18 h	26 h	4 h	20 h	96 h	192 h	288 h
4 h	12 h	20 h		8 h	24 h	120 h	216 h	
6 h	14 h	22 h		12 h	48 h	144 h	244 h	
8 h	16 h	24 h		16 h	72 h	168 h	264 h	

Curve fitting and growth parameters estimation

Growth curves were fitted to Baranyi and Roberts primary predictive model [19] (Equations 1-3), using DMFit online (Quadram Institute, Norwich, United Kingdom), to estimate maximum specific growth rate (μ_{max}), lag time (λ), initial and final concentration (C_0 and C_f, respectively); R-square (R^2) and standard error of fit (SE) were used to evaluate the performance of the models built in this study. A fitting method for repeated measures was applied considering the different replicates analyzed in each time point.

$$(1) \quad N(t) = N_0 + \mu_{max} A(t) - ln\left[1 + \frac{e^{\mu_{max} A(t)} - 1}{e^{(N_{max} - N_0)}}\right]$$

$$(2) \quad A(t) = t + \frac{1}{\mu_{max}} ln\left(\frac{e^{(-\mu_{max} t)} + q_0}{1 + q_0}\right)$$

$$(3) \quad \lambda = \frac{ln\left(1 + \frac{1}{q_0}\right)}{\mu_{max}}$$

Where: N(t)= log of cell concentration (cfu/ml(g)) at time t (h); N0= log of initial cell concentration (cfu/ml(g)); μmax= maximum specific growth rate (log cfu/ml(g)/h); Nmax= log of maximum cell concentration; q0= parameter expressing the physiological state of cells when t= t0; λ= lag time (h). In this work, μmax was based on the inflection of the growth curve slope in the exponential phase [20].

The resulting growth curves and parameters were compared to predicted values generated by ComBase Predictor Growth Model (ComBase, Hobart, Australia). ComBase model was run with the following selected parameters: Initial level= 4.5 log cfu/ml; pH= 7.4 and a_w= 0.997 were BHI broth data.

Calibration curves

To study OD_{600nm} and cell count (cfu/ml) relation, calibration curves were prepared. For that, L. *monocytogenes* CECT 4031 were cultured on BHI agar (Scharlab, S.B.) for 18 h at 37°C. Afterwards, cultures were transferred to 10 ml of tryptone salt broth (Scharlab, S.B.), resulting in a suspension with an OD_{600nm} of 0.4 – 0.5 and serial dilutions were prepared. Serial dilutions OD_{600nm} were measured and correlated with cfu/ml obtained in plate counts on BHI agar (Scharlab, S.B.). This assay was performed in triplicate.

Biofilm formation assay

The protocol proposed by Romanova, Gawande, Brovko and Griffiths [21] was used with some modifications to obtain a 5-day L. *monocytogenes* mono-cultural biofilm. A single colony of each selected strain was inoculated in Buffered Peptone Water (BPW) (Scharlab, S.B), incubating overnight at 30°C. Bacterial suspension OD_{600nm} was adjusted to 0.1 approximately, in Ultrospec 2000 (Pharmacia Biotech), to obtain a concentration of 8 log cfu/ml, according to the above mentioned calibration curve. For each strain, 4 μl were transferred into three separate wells of polystyrene flat-bottomed microtiter plates (Normax, Marinha Grande, Portugal) filled with 200 μl of BPW. Three wells were used as negative controls, containing only BPW. The plates were statically incubated at 30°C for 5 days. The solution was then removed from the wells that were rinsed with sterile distilled water to remove loosely associated bacteria and the attached biofilms were evaluated by Viable Cells Counts (VCC) and Crystal violet staining (cvOD). This assay was performed in triplicate, with three replicates for each strain. L. *monocytogenes* CECT 4031 and CECT 935 were further assess for biofilm formation at 12°C and 20°C. For that, the abovementioned procedure was followed and the plates were statically incubated at 12°C and 20°C for 5 days.

Biofilm assessment by viable cells counts

The biofilm was detached from the well surface with 100 μl of BPW using a mini cell scraper and sonicated (Ultrasonic bath MXB14, Grant Instruments, England) for 5 min to detach and collect sessile cells. Another 100 μl of BPW were pipetted into each well, serial 10-fold dilutions were prepared and 10 μl samples were dropped onto the surface of a Tryptone Soy Agar (TSA) (Scharlab, S.B) plate. Colonies were enumerated after overnight incubation at 30°C in a stereoscopic magnifier (Nikon SMZ645, Tokyo, Japan).

Biofilm assessment by crystal violet staining

The microtiter plate was left air drying for 45 min in the laminar flow hood. Biofilm was stained using 220 μl of of 0.1% crystal violet (bioMérieux, France) solution for 15 min at room temper-ature. After stain removal, the wells were washed three times with sterile distilled water and left air drying for 30 min in the laminar flow hood. To quantify adhered cells, 220 μl of detaining solution (ethanol: Acetone 80:20 v/v) were added to each well for 15 min at room temperature. The microtiter plate was then shaken (Ultrasonic bath MXB14, Grant) for 5 min and the Crystal Violet OD (cvOD) was measured in SpectraMax 340PC (Molecular Devices, California, USA). Each absorbance value was corrected by subtracting the average absorbance readings of the blank control wells.

Adherence capability was based on the cvOD exhibited by bacterial biofilms, according to Stepanović, Cirković, Ranin, and Svabić-Vlahović [22]. The cut-off cvOD (cvODc) was defined as three standard deviations above the negative control mean cvOD. The strains were classified as no biofilm producers (cvOD ≤ ODc), weak biofilm producers (cvODc ≤ OD ≤ 2 x ODc), moderate biofilm producers (2 x cvODc ≤ cvOD ≤ 4 x cvODc) and strong biofilm producers (4 x cvODc < cvOD).

Data analyses

All quantitative data are presented as mean values with Standard Deviation (SD) from three independent experiments.

OD_{600nm} and VCC data were used to fit a linear regression in Microsoft Excel 2016 software (Microsoft Corporation, Redmond, USA).

Pearson's correlation analysis was performed in GraphPad software Prism 5 (GraphPad Software, La Jolla, USA) to relate OD_{600nm} and experimental VCC values.

The calibration curve was obtained from the following equation:

(4)   cfu/ml = slope × OD600nm + interception.

For L. *monocytogenes* growth characterization, VCC experimental results were adjusted using DMFit Online (Quadram Institute, Norwich, United Kingdom), which was also used to estimate growth related parameters.

To assess L. *monocytogenes* biofilm formation parameters at different temperatures (12°C, 20°C and 30°C), Pearson's correlation analyses were used to evaluate the interdependency of cvOD and VCC. Two-way ANOVA was used to investigate the temperature effect on biofilm formation.

Results & discussion

Listeria monocytogenes isothermal growth in BHI broth

Growth rates of L. *monocytogenes* were studied at different temperatures in a defined medium (BHI). L. *monocytogenes* CECT 4031 was chosen since it is the type strain for this specie [23].

The selected temperatures were 37°C, corresponding to L. *monocytogenes*' optimal growth temperature [24,25], and 12°C, which is used in food producing rooms at industrial facilities [26].

Figure 1 shows the resulting growth curves based on L. *monocytogenes* CECT 4031 OD_{600nm} values in BHI at each sampling time point, incubated for 26 hours at 37°C (A) and for 12 days at 12°C (B).
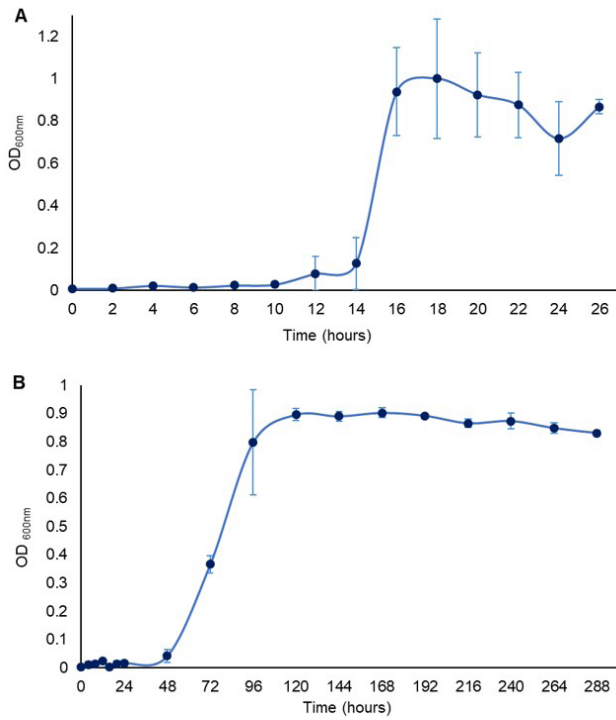
Figure 1: Growth curves of *L. monocytogenes* CECT 4031 at **(A)** 37°C for 26h, and **(B)** at 12°C for 12 days, obtained from average and standard deviation (error bars) of OD_{600nm} measurements.

L. *monocytogenes* CECT 4031 growth occurred at both temperatures, although differences were observed (Figure 1). At 37°C a lag phase of approximately 10 hours was observed, followed by an exponential growth phase from 10 h to 18 h. From then on until the end of the incubation time (26 h), stationary phase was observed. The maximum OD_{600nm} value was 0.999 ± 0.280 at 18 h. Mytilinaios et al. (2012), when studying growth rate of L. *monocytogenes* in tryptone soya broth at 37°C, obtained an average maximum optical density of 0.99.

At 12°C the lag phase lasted approximately 48 hours, and from 48 h to 120 h the exponential growth phase was observed. Stationary phase seems to have been reached at 120 hours. The maximum OD_{600nm} value was 0.902 ± 0.017 at 168 h.

Figure 2 presents the obtained growth curves for L. *monocytogenes* CECT 4031 in BHI considering total Viable Cell Counts (VCC) for the assessed sampling time points, at 37°C (A) and at 12°C (B).

At 37°C, a stationary phase can be observed in the first 18 h of incubation, however the maximum value of VCC 9.484 ± 0.678 log cfu/ml was obtained at 26h. At 12°C, there seems to be a potential lag phase of approximately 48 hours, and from 48 h to 120 h the exponential growth phase can be observed. Stationary phase seems to have been reached at 120 hours after inoculation. The maximum value of VCC reached was 9,277 ± 0,210 log cfu/ml at 168 h. Castro [26] obtained similar results when studying the growth of L. *monocytogenes* in packaged raw milk, in which, from initial low counts, L. *monocytogenes* was able to develop to 4.3 ± 0.4 log cfu/ml at refrigerated temperatures (10°C).

Temperature had a considerable influence on L. *monocytogenes* growth, because although initial and final concentrations are similar for both temperatures, the time needed to reach final concentration was higher for the lower temperature (12°C). In order to reach approximate maximum concentrations, around 18/20 hours were needed at 37°C and 5/6 days at 12°C. This was observed when applying both OD_{600nm} and VCC measurements.

The correlation curves obtained for L. *monocytogenes* 4031 using OD_{600nm} and VCC are shown in Figure 3A (37°C) and Figure 3B (12°C).
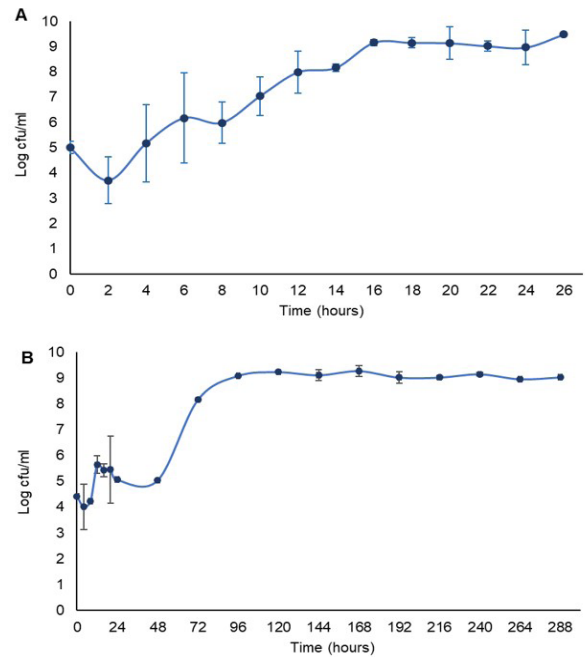
Figure 2: Growth curves of *L. monocytogenes* CECT 4031 at **(A)** 37°C for 26h, and **(B)** at 12°C for 12 days, obtained from average and standard deviation (error bars) of viable cell counts.

$$y = 3.6192x + 5,9794$$
$$R^2 = 0.6929$$

$$y = 4.8789x + 4,9406$$
$$R^2 = 0.9372$$
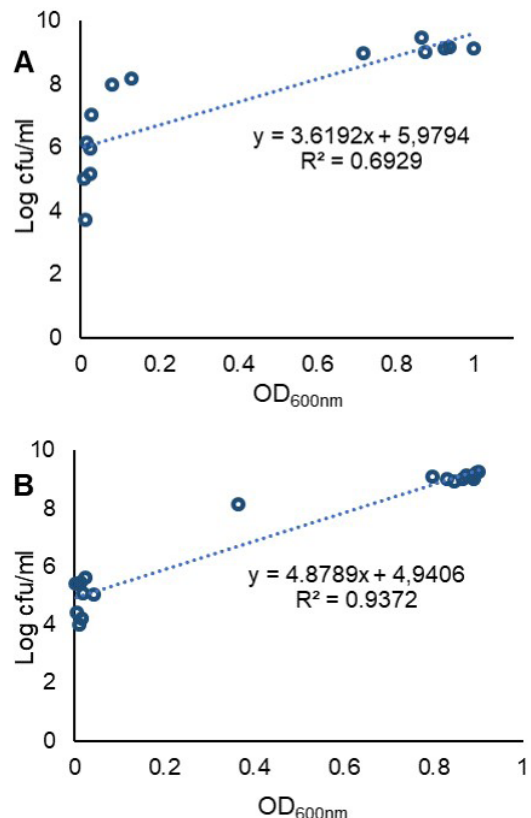
Figure 3: Scattered plot of experimental OD_{600nm} and VCC for *L. monocytogenes* CECT 4031 at **(A)** 37°C and **(B)** 12°C.

When comparing experimental OD_{600nm} and VCC results (Table 2), although a good correlation was observed between both methods, Pearson correlation and R^2 were higher at 12^{0}C.

Table 2: Correlation analysis between OD_{600nm} measurements and VCC.

Temperature	Pearson correlation	95% confidence interval (IC)	R^2
37ºC	0.8324	0.5404 to 0.9454	0.6929
12ºC	0.9681	0.9145 to 0.9883	0.9372

At 37°C, the R^2 value (0.6929) revealed a low adjustment/fit when using OD_{600nm} to estimate VCC. This difference may be related to the fact that optical density measures the turbidity of a suspension, and because of that its relationship with cell concentration may not be linear (deposits of non-viable cells in suspension are also measured as total number of cells). Some authors defend that the difference between both methods is especially evident when assessing growth parameters of isolates in stressful conditions, as morphological changes in the cell may result in optical density values that do not reflect the actual cell numbers [27-29]. Jones, Gill, and McMullen [30] showed that cold adaptation can sometimes cause cell elongation, as cells further increase in cell length before dividing to normal cell length, strongly affecting the relationship between the optical density levels reached and the estimated log cfu/ml.

Nonetheless, the correlation of both methods was high, indicating that VCC values can be reliably inferred through optical density measurements with the use of calibration equations, delivering fast and effective results.

Curve fitting and growth parameters estimation

For each temperature and using VCC values, growth curves were built by fitting experimental data to the Baranyi's DMFit *online* version.
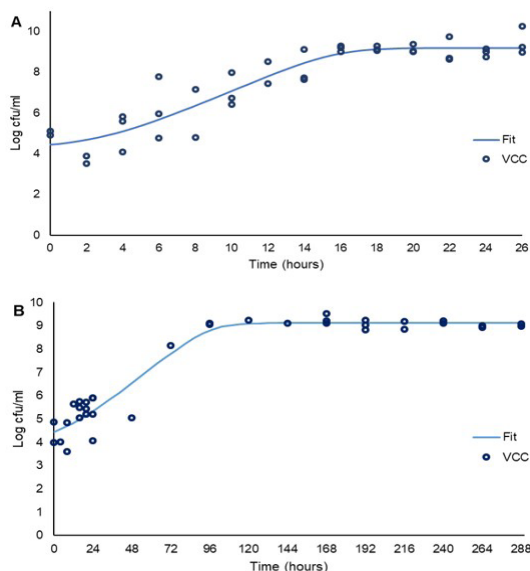
Figure 4: L. *monocytogenes* CECT 4031 VCC (log cfu/ml) fitted with Baranyi and Roberts model. (A) Incubation for 26 hours at 37°C (R^2: 0.845; SE: 0.748). (B) Incubation for 12 days at 12°C (R^2: 0.937; SE: 0.530).

At 37°C, L. *monocytogenes* CECT 4031 concentration peaked at 21h reaching 9.184 ± 0.204 log cfu/ml (Figure 4A) and remaining stable until the end of incubation time (stationary phase). At 12°C, L. *monocytogenes* CECT 4031 reached a maxi-

mum final concentration of 9.117 ± 0.133 log cfu/ml after 144 h (Figure 4B) and remained stable until the end of incubation time (stationary phase).

The obtained R^2 results for both temperatures revealed a good fit of the model to experimental data.

Table 3: Maximum growth rate (μ_{max}), lag time (λ), initial (C_0) and final (C_f) concentrations (mean ± SD) for L. *monocytogenes* CECT 4031 estimated by DMFit Model using VCC results, at 37°C and 12°C.

Temperature	μ_{max} (log cfu/ml/h)	λ (h)	C_0 (log cfu/ml)	C_f (log cfu/ml)
37°C	0.375 ± 0.072	3.026 ± 2.263	4.446 ± 0.436	9.184 ± 0.204
12°C	0.054 ± 0.001	9.856 ± 11.681	4.454 ± 0.289	9.117 ± 0.133

Considering the obtained estimated growth parameters (Table 3), μ_{max} at 37°C was higher than at 12°C, and a longer lag phase was observed at this temperature (12°C). The longer lag phase at 12°C could be due to an adaptation period to lower temperatures. Similar growth parameters were obtained by Pla [31], when assessing L. *monocytogenes* CECT 4031 growth in Tryptic soy broth supplemented with 0.6% yeast extract at 37ºC (μ_{max} = 0.447 and λ = 1.86), and by Wang [32] when studying the growth of L. *monocytogenes* in BHI at 10ºC (μ_{max} = 0.066 and λ = 17 h).

More time was needed for L. *monocytogenes* to grow at 12°C and reach the same concentrations as those obtained at 37°C. However, final concentrations of the pathogen were very similar, emphasizing the ability of L. *monocytogenes* to grow at refrigerated temperatures, as the ones used in food producing rooms at industrial facilities. In fact, after 5/6 days of incubation at 12°C, the levels of L. *monocytogenes* were similar to the ones reached at 37°C.

Predictions obtained from Baranyi's model using L. *monocytogenes* VCC at both temperatures were compared to the estimated growth using ComBase Predictor Growth model (Figure 5).
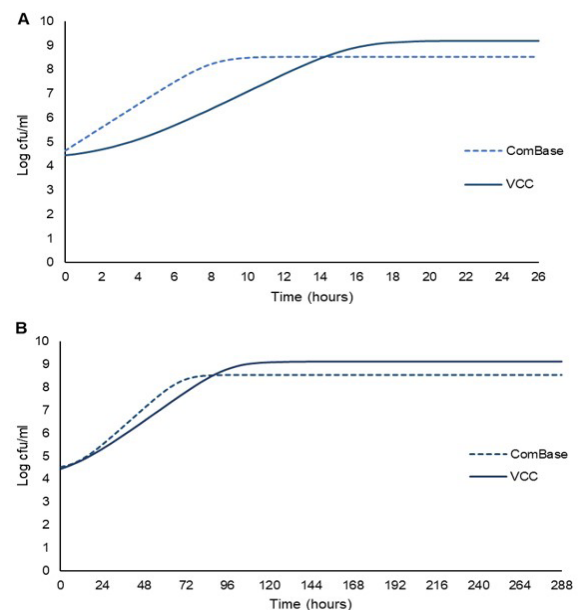
Figure 5: Comparison of L. *monocytogenes* fitted growth curves obtained from VCC and the online software Combase Predictor Growth Model at **(A)** at 37°C for 26 h and **(B)** at 12°C for 12 days.

In general, predictions from ComBase Predictor growth model and this study's results were quite similar. However, when considering the temperature of 37°C, the growth curve based on VCC presented lower values until 14 h of incubation, but higher maximum values when compared with ComBase estimated growth curve. The stationary phase was reached sooner in ComBase estimated growth curve. Also, μ_{max} obtained with ComBase predictor was of 0.480 log cfu/ml/h, higher when compared to the experimental data μ_{max} (0.375 ± 0.072 log cfu/ml/h, Table 3).

At 12°C, the stationary phase was reached later in the estimated growth curve based on VCC. ComBase growth curve presents lower maximum log cfu/ml values. Considering the maximum growth rate (μ_{max}) obtained with ComBase predictor, at 12°C a μ_{max} of 0.068 log cfu/ml/h was estimated, which was higher than the experimental data μ_{max} (0.054 ± 0.001 log cfu/ml/h, Table 3).

Calibration curves

A calibration equation for each strain in the study was obtained by performing three independent calibration curves, in which viable cell counts were plotted against OD_{600nm} data (Figure 6), allowing a given concentration (cfu/ml) to be determined from the OD_{600nm} value assessed using a spectrophotometer.
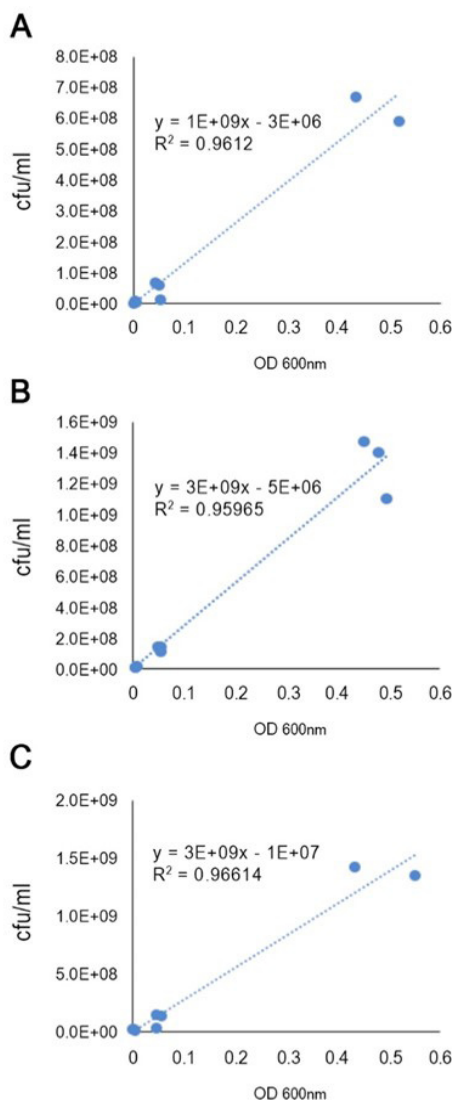
Figure 6: Plot of the observed OD_{600nm} against the VCC (cfu/ml) for **(A)** *Listeria monocytogenes* CECT 4031, **(B)** *Listeria monocytogenes* CECT 935 and **(C)** *Listeria monocytogenes* CECT 937. Each value corresponds to the mean of three replicates.

Regression parameters and goodness of fit (R^2) of the calibration curve are shown in Table 4.

Table 4: Main statistical parameters for the regression curve obtained for L. *monocytogenes* strains' calibration curves.

L. *monocytogenes* strain	Slope	Intercept	R^2 adjusted
CECT 4031	1×10^9	3×10^6	0.9987
CECT 935	3×10^9	5×10^6	0.9597
CECT 937	3×10^9	1×10^7	0.9661

Results indicate a high correlation between OD_{600nm} values and cfu/ml (coefficient of determination, R^2= 0.9987), which indicates that the method is reliable for quantifying L. *monocytogenes* strains. Pearson's correlation coefficient indicates a strong positive correlation between cfu/ml and OD_{600nm} (ρ = 0.9994, p < 0.0001). Similar results were obtained by Ripolles-Avila [33] for L. *monocytogenes* CECT 935.

Biofilm formation assay

The assessed strains in biofilms revealed cvOD values ranging from 0.068 ± 0.001 to 0.1078 ± 0.005 and viable cell counts of 6.013 ± 0.346 log cfu/ml to 7.391 ± 0.227 log cfu/ml after 5 days of growth in polystyrene microtiter wells (Figure 7).

According to Stepanović, Cirković, Ranin, and Svabić-Vlahović [22] classification, all the strains revealed a weak biofilm- forming ability. Meloni [25] obtained similar results when studying L. *monocytogenes* isolates from fermented sausage processing plants: 65% of all isolates were weak biofilm producers.

While L. *monocytogenes* CECT 4031 revealed the lowest values for both VCC and cvOD at 30°C, L. *monocytogenes* CECT 935 exhibited the highest biofilm-forming ability, based on both biofilm formation parameters. Similar results were obtained by Ripolles-Avila [33] when studying the quantification of cell density within L. *monocytogenes* biofilms based on cvOD.
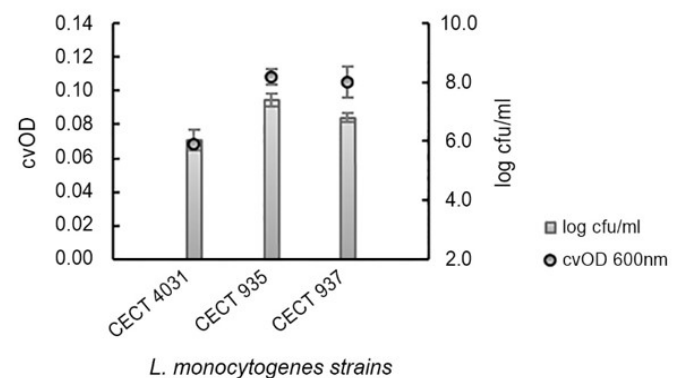
Figure 7: Average and standard deviation of log cfu/ml and cvOD of the assessed 5-day L. *monocytogenes* biofilms at 30°C.

Considering the selected methods to analyse biofilm formation - VCC (log cfu/ml) and cvOD, a positive and strong correlation (ρ= 0.7749, p= 0.009) was obtained. This coefficient value indicates that both methods presented a good relation, being reliable to quantifying L. *monocytogenes* biofilm formation and complementing each other.

Differences between cvOD and VCC results are due to the nature of each method determination: While cvOD measures the turbidity of a suspension and quantifies total biomass (via-

ble and non-viable cells, and extracellular matrix components), VCC only considers live cells [34]. Although monitoring biofilm formation with VCC is time-consuming, laborious and expensive because the technique is based on serial dilutions and plating methods, it remains the method of reference for monitoring bacterial growth [27,29,35]. On the other hand, cvOD method may overestimate the number of viable, attached cells [34,36]. Additionally, stressful conditions may induce morphological changes in cells, such as cell elongation, strongly affecting the relationship between cvOD and VCC [29].

For further testing, L. *monocytogenes* CECT 935 and CECT 4031 were selected based on Tukey's test results for VCC and cvOD, that presented statistically significant differences (p < 0.05) in both biofilm formation parameters.
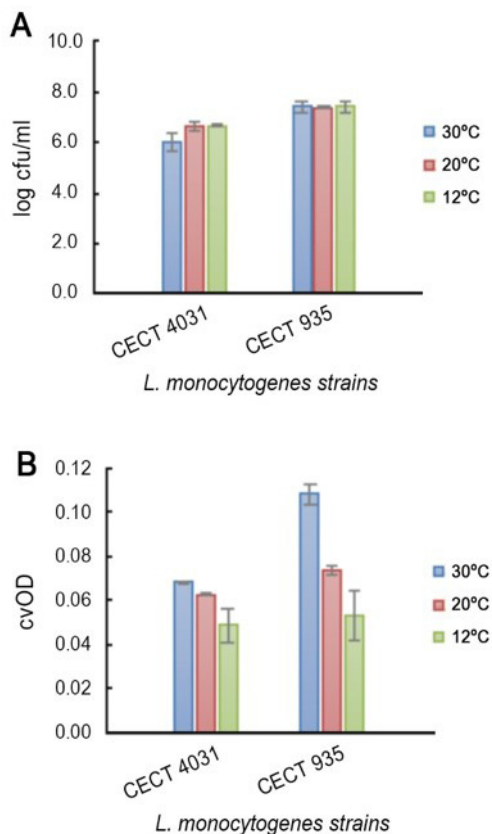
Figure 8: Average and SD (error bars) of the selected L. *monocytogenes* strains in 5-day old biofilms considering **(A)** Viable cells counts (log cfu/ml) and **(B)** Crystal Violet staining (cvOD).

All of the tested L. *monocytogenes* isolates were able to form biofilm at 30°C, 20°C and 12°C (Figure 8). Although there were no significant differences (p= 0.958) in biofilm formation at different temperatures considering VCC values (Figure 8A), using cvOD (Figure 8B) significant differences (p= 0.0002) were observed in biofilm formation for the considered temperatures.

It is important to underline that the studied L. *monocytogenes* strains revealed biofilm-forming ability at refrigerated processing environment temperatures (12°C and 20°C), as the ones used in refrigerated producing rooms in the food industry. Still, the highest biofilm formation occurred at 30°C for all L. *monocytogenes* tested strains, confirming that temperature influences L. *monocytogenes* biofilm formation, as has been previously reported. Tomičić [37] reported that growth conditions affected biofilm formation, revealing the lowest biofilm formation for the lowest tested temperature. Similar results were obtained by Russo [2] when testing L. *monocytogenes* biofilm-forming ability on polystyrene under different temperatures. In fact, Abeysundara [38] observed that biofilm formation was influenced by temperature, resulting in decreased biofilm formation with decreasing temperature. Di Bonaventura [39] demonstrated that biofilm production on polystyrene surfaces at 37°C was significantly higher than at 4°C. However, according to Puga [40], some evidence suggests that persistence of certain strains may be enhanced by low temperatures adaptation mechanisms. Temperature may influence flagella formation actively involved in the adhesion to different surfaces [2].

Conclusions

In this study, when fitting planktonic L. *monocytogenes* isothermal growth experimental data to Baranyi's model, a good fit was obtained for both temperatures. The estimated growth parameters confirmed that μmax at 37°C was higher than at 12°C, and a longer lag phase was observed at this temperature, indicating an adaptation period to lower temperatures. Still, L. *monocytogenes* final concentrations were identical, emphasizing its ability to grow at refrigerated temperatures. Additionally, experimental results from the isothermal growth assay and ComBase Predictor growth model were rather similar, but higher μmax were estimated for both temperatures by the predictor model.

Calibration curves using OD_{600nm} and VCC results indicated a strong positive correlation of both parameters, confirming the reliability of both parameters to estimate L. *monocytogenes* concentration.

The studied L. *monocytogenes* strains demonstrated biofilm-forming ability at 12°C, 20°C and 30°C after 5 days of growth and all revealed to be weak biofilm producers. Although there were no significant differences in biofilm formation at different temperatures considering VCC values, using cvOD significant differences were found and the highest biofilm formation occurred at 30°C.

Still, a positive and strong correlation was found between VCC and cvOD results, which complement each other in biofilm formation assessment.

Overall, this study's outcomes contribute with important preliminary data on L. *monocytogenes* growth at different temperatures, whether in the planktonic form or in biofilms. The gathered data will further assist predictive modeling and risk assessment studies, improving possible interventions and mitigation strategies to control this important foodborne pathogen.

References

1. European Food Safety Authority (EFSA) and European Centre for Disease Prevention and Control (ECDC). The European Union One Health 2018 Zoonoses Report. EFSA J. 2019; 17: 5926.

2. Russo P, Hadjilouka A, Beneduce L, Capozzi V, Paramithiotis S, et al. Effect of different conditions on Listeria monocytogenes biofilm formation and removal. Czech J Food Sci. 2018; 36: 208–214.

3. Sahu SN, Kim B, Ferguson M S, Zink D L, Datta A R. Growth potential of Listeria monocytogenes in artificially contaminated celery and chicken salad. Food Control. 2016; 73: 1229–1236.

4. Listeriosis DS: A Rare but Deadly Disease. Clin Microb Newsl. 2015; 37 (17): 135-140.

5. Buchanan RL, Gorris LGM, Hayman MM, Jackson TC, Whiting RC. A review of Listeria monocytogenes: An update on outbreaks, virulence, dose-response, ecology, and risk assessments. Food Control. 2017; 75: 1–13.

6. Li C, Huang L, Hwang CA, Chen J. Growth of Listeria monocytogenes in salmon roe - A kinetic analysis. Food Control. 2016; 59: 538–545.

7. Henriques AR, Fraqueza MJ. Listeria monocytogenes: Incidence, Growth Behavior and Control. New York, NY, USA: Nova Science Publishers Inc. 2015; 71–103.

8. Olszewska MA, Zhao T, Doyle MP. Inactivation and induction of sublethal injury of Listeria monocytogenes in biofilm treated with various sanitizers. Food Control. 2016; 70: 371–379.

9. Bonsaglia ECR, Silva NCC, Fernandes JA, Araújo Junior JP, Tsunemi MH, et al. Production of biofilm by Listeria monocytogenes in different materials and temperatures. Food Control. 2014; 35: 386–391.

10. Kannan S, Balakrishnan J, Govindasamy A. Listeria monocytogenes - Amended understanding of its pathogenesis with a complete picture of its membrane vesicles, quorum sensing, biofilm and invasion. Microb Pathog. 2020; 149: 104575.

11. Allen KJ, Wałecka-Zacharska E, Chen JC, Katarzyna K-P, Devlieghere F, et al. Listeria monocytogenes – An examination of food chain factors potentially contributing to antimicrobial resistance. Food Microbiol. 2016; 54: 178-189.

12. Ortiz S, López V, Martínez-Suárez JV. Control of Listeria monocytogenes contamination in an Iberian pork processing plant and selection of benzalkonium chloride-resistant strains. Food Microbiol. 2014; 39: 81–88.

13. Szczawiński J, Szczawińska ME, Łobacz A, Tracz M, Jackowska-Tracz A. Modelling the growth rate of Listeria monocytogenes in cooked ham stored at different temperatures. J Vet Res. 2017; 61: 45–51.

14. Chen R, Skeens J, Orsi RH, Wiedmann M, Guariglia-Oropeza V. Pre-growth conditions and strain diversity affect nisin treatment efficacy against Listeria monocytogenes on cold-smoked salmon, Int J Food Microbiol. 2020; 333: 108793.

15. Bernardo R, Barreto AS, Nunes T, Henriques AR. Estimating Listeria monocytogenes Growth in Ready-to-Eat Chicken Salad Using a Challenge Test for Quantitative Microbial Risk Assessment. Risk Anal. 2020.

16. Tirloni E, Stella S, de Knegt LV, Gandolfi G, Bernardi C, et al. A quantitative microbial risk assessment model for Listeria monocytogenes in RTE sandwiches. Microb Risk Anal. 2018; 9: 11–21.

17. Álvarez-Ordóñez A, Leong D, Hickey B, Beaufort A, Jordan K. The challenge of challenge testing to monitor Listeria monocytogenes growth on ready-to-eat foods in Europe by following the European Commission (2014) Technical Guidance document. Food Res Int. 2015; 75: 233–243.

18. Takahashi H, Takahashi T, Miya S, Yokoyama H, Kuda T, et al. Growth inhibition effects of ferulic acid and glycine/sodium acetate on Listeria monocytogenes in coleslaw and egg salad. Food Control. 2015; 57: 105–109.

19. Baranyi J, Roberts TA. A dynamic approach to predicting bacterial growth in food. Int J Food Microbiol. 1994; 23: 277–294.

20. Baranyi J, Roberts TA, McClure P. A non-autonomous differential equation to model bacterial growth. Food Microbiol. 1993; 10: 43–59.

21. Romanova NA, Gawande PV, Brovko LY, Griffiths, MW. Rapid methods to assess sanitizing efficacy of benzalkonium chloride to Listeria monocytogenes biofilms. J. Microbiol. Methods. 2007; 71: 231–237.

22. Stepanović S, Cirković I, Ranin L, Svabić-Vlahović M. Biofilm formation by Salmonella spp. and Listeria monocytogenes on plastic surface. Lett. Appl. Microbiol. 2004; 38: 428–432.

23. Davenport KW, Daligault HE, Minogue TD, Bishop-Lilly TA, Bruce DC, P. et al. Whole-Genome Sequence of Listeria monocytogenes Type Strain 53 XXIII. Genome Announc. 2014; 2: e00970-14.

24. Beaufort A, Bergis H, Lardeux AL. Technical guidance document for conducting shelf-life studies on Listeria monocytogenes in ready-to-eat foods. European Union Reference Laboratory for Listeria monocytogenes. 2014; 3: 1–47.

25. Meloni D, Consolati SG, Mazza R, Mureddu A, Fois F, et al. Presence and molecular characterization of the major serovars of Listeria monocytogenes in ten Sardinian fermented sausage processing plants. Meat Sci. 2014; 97: 443–450.

26. Castro H, Ruusunen M, Lindström M. Occurrence and growth of Listeria monocytogenes in packaged raw milk. Int J Food Microbiol. 2017; 261: 1–10.

27. Baty F, Flandrois JP, Delignette-Muller ML. Modeling the lag time of Listeria monocytogenes from viable count enumeration and optical density data. App Environ Microbiol. 2002; 68: 5816–5825.

28. Bereksi N, Gavini F, Bénézech T, Faille C. Growth, morphology and surface properties of Listeria monocytogenes Scott A and LO28 under saline and acid environments. J Appl Microbiol. 2002; 92: 556-65.

29. Francois K, Devlieghere F, Standaert A, Geeraerd A, Cools I, et al. Environmental factors influencing the relationship between optical density and cell count for Listeria monocytogenes. J Appl Microbiol. 2005; 99: 1503-1515.

30. Jones T, Gill CO, McMullen LM. Behaviour of log-phase Escherichia coli at temperatures near the minimum for growth. Int J Food Microbiol. 2003; 88: 55–61.

31. Pla ML, Oltra S, Esteban MD, Andreu S, Palop A. Comparison of Primary Models to Predict Microbial Growth by the Plate Count and Absorbance Methods. BioMed Res Int. 2015; 365025.

32. Wang X, Lahou E, De Boeck E, Devlieghere F, Geeraerd A, et al. Growth and inactivation of Salmonella enterica and Listeria monocytogenes in broth and validation in ground pork meat during simulated home storage abusive temperature and home pan-frying. Front Microbiol. 2015; 6: 1161.

33. Ripolles-Avila C, Ríos Castillo AG, Guerrero-Navarro AE, Rodrí-guez-Jerez JJ. Reinterpretation of a classic method for the quantification of cell density within biofilms of Listeria monocytogenes. J Microbiol Exp. 2018; 6: 70–75.

34. Ibusquiza PS, Herrera JJR, Cabo ML. Resistance to benzalkonium chloride, peracetic acid and nisin during formation of mature biofilms by Listeria monocytogenes. Food Microbiol. 2011; 28: 418–425.

35. Kwasny SM, Opperman TJ. Static biofilm cultures of Gram-positive pathogens grown in a microtiter format used for anti-biofilm drug discovery. Curr Protoc Pharmacol. 2010; 13: 13A8.

36. Kadam SR, den Besten HM, van der Veen S, Zwietering MH, Moezelaar R, et al. Diversity assessment of Listeria monocytogenes biofilm formation: Impact of growth condition, serotype and strain origin. Int J Food Microbiol. 2013; 165: 259–264.

37. Tomiĉić R, Cabarkapa I, Vukmirovic D, Tomiĉić Z. Influence of growth conditions on biofilm formation of Listeria monocytogenes. Food Feed Res. 2016; 43: 19-24.

38. Abeysundara PA, Dhowlaghar N, Nannapaneni R, Schilling MW, Chang S, et al. Growth and biofilm formation by Listeria monocytogenes in cantaloupe flesh and peel extracts on four food-contact surfaces at 22 °C and 10 °C. Food Control, 2017; 80: 131-142.

39. Di Bonaventura G, Piccolomini R, Paludi D, D'Orio V, Vergara A, et al. Influence of temperature on biofilm formation by Listeria monocytogenes on various food-contact surfaces: Relationship with motility and cell surface hydrophobicity. J Appl Microbiol. 2008; 104: 1552–1561.

40. Puga CH, SanJose C, Orgaz B. Biofilm development at low temperatures enhances Listeria monocytogenes resistance to chitosan. Food Control. 2016; 65: 143–151.